3D Bioprinting of Diatom-Laden Living Materials for Water Quality Assessment

Rani Boons, Gilberto Siqueira,* Florian Grieder, Soo-Jeong Kim, Diego Giovanoli, Tanja Zimmermann, Gustav Nyström,* Fergal B. Coulter, and André R. Studart*

Diatoms have long been used as living biological indicators for the assessment of water quality in lakes and rivers worldwide. While this approach benefits from the great diversity of these unicellular algae, established protocols are time-consuming and require specialized equipment. Here, this work 3D prints diatom-laden hydrogels that can be used as a simple multiplex bio-indicator for water assessment. The hydrogel-based living materials are created with the help of a desktop extrusion-based printer using a suspension of diatoms, cellulose nanocrystals (CNC) and alginate as bio-ink constituents. Rheology and mechanical tests are employed to establish optimum bio-ink formulations, whereas cell culture experiments are utilized to evaluate the proliferation of the entrapped diatoms in the presence of selected water contaminants. Bioprinting of diatom-laden hydrogels is shown to be an enticing approach to generate living materials that can serve as low-cost bio-indicators for water quality assessment.

1. Introduction

Living materials rely on the metabolic activity of microorganisms to achieve self-healing, regenerative and adaptive functionalities not found in their synthetic counterparts.[1–6] Examples include self-healing concrete,[7,8] cell-regulated adhesive hydrogels,[5,9] and regenerative mycelial networks.[10] Such functionalities emerge from microorganisms that are able to directly grow, secrete or induce the formation of materials as part of their natural metabolism or engineered genome. The metabolism of soil bacteria has been exploited to induce the precipitation of calcium carbonate in self-healing concrete,[7,8] whereas fungi has been used to grow mycelial networks for regenerating robotic skins.[10] Alternatively, *E. coli* can be genetically engineered to enable light-triggered chemical release[9] or to secrete curli fibers that promote cell and tissue adhesion.[5] The advanced synthetic biology tools currently available for genetic engineering and the broad diversity of microbial species that produce extracellular materials provide a vast range of opportunities in the field of engineered living materials.

While material-secreting bacterial communities in nature form biofilms through bottom-up cellular processes, top-down 3D bioprinting is an effective approach to controllably shape wild and genetically programmed microorganisms into living materials with complex, multi-species architecture.[1,11–13] This strategy has been applied to create living materials loaded with cellulose-producing bacteria,[1,14] photosynthetic algae,[12,15,16] bioluminescent bacteria,[13] catalytically active yeast,[17] and engineered *E. coli*[11] using light- or extrusion-based bioprinting technologies.[18] Since direct ink writing, also known as extrusion bioprinting, offers multi-material capabilities and operates at room temperature, it is an attractive extrusion-based process for the 3D bioprinting of bacteria-laden hydrogels.[1,11,19] To ensure cell viability and shape retention, bio-ink formulations usually contain biocompatible polymers and rheology modifiers combined with the microorganism of interest. Although the bio-ink composition often needs to be tuned to match the needs of specific microbial species, universal biocompatible hydrogels are available for the formulation of bio-inks with a broad variety of natural or engineered microorganisms.[1,20]

Diatoms are particularly interesting in this context because these microorganisms consist of photosynthetic unicellular algae that produce exquisite silica exoskeletons[21] and play a major ecological role in nature.[22] With sizes ranging from 1 μm to a few millimeters, these microorganisms are found in

R. Boons, G. Siqueira, T. Zimmermann, G. Nyström
Cellulose & Wood Materials Laboratory
Empa
Swiss Federal Laboratories for Materials Science and Technology
Dübendorf 8600, Switzerland
E-mail: gilberto.siqueira@mat.ethz.ch; Gustav.Nystroem@empa.ch
R. Boons, G. Siqueira, F. Grieder, S.-J. Kim, D. Giovanoli, F. B. Coulter, A. R. Studart
Complex Materials
Department of Materials
ETH Zurich
Zurich 8093, Switzerland
E-mail: andre.studart@mat.ethz.ch
G. Nyström
Department of Health Sciences and Technology
ETH Zürich
Zürich 8092, Switzerland

massive concentrations in most waterbodies.[22,23] Evolution over 250 million years has led to the diversification of diatoms into ≈200 000 different species, each characterized by different appearances and adaptations to their specific habitat.[24] Because of their widespread and photosynthetic nature, diatoms are estimated to be responsible for about 20 – 25% of earth's oxygen production.[25] The omnipresence of diatoms in lakes and rivers combined with their sensitivity to waterborne contaminants has made them useful bio-indicators for water quality assessment.[26,27] Indeed, several indices are currently used to assess water quality by analysing the distribution of diatom species of different sensitivities present in freshwater sources.[27–29] However, this approach is still time-consuming and requires specialized infrastructure and expertise for implementation and analysis.[30] Engineering a living material that harnesses the metabolism of diatoms to detect waterborne contaminants could potentially lead to cost-effective and ready-to-use bio-indicators for water quality assessment.

Here, we develop and study a 3D bioprinting platform for the creation of hydrogels loaded with living diatoms that can be used as bio-indicators for water quality control. The bio-indicators are printed from hydrogel feedstock containing distinct diatom species using a multi-material extrusion bioprinting technique. First, we investigate and quantify the effect of the ink composition on the rheological behavior, printability, mechanical properties and cell growth in the hydrogels. An optimized bio-ink formulation is then used to bioprint samples with two selected diatom species, which were tested in terms of sensitivity to typical water contaminants. Finally, we print multiplex bio-indicators with different architectures and compare their ability to detect the presence of waterborne chemicals using microscopy imaging or visual color changes as sensing readouts.

2. Results and Discussion

3D bioprinting of the living bio-indicator is carried out through four main steps: bio-ink preparation using selected diatoms, extrusion bioprinting of the device, diatom proliferation and water assessment (**Figure 1**). First, diatoms species that are sensitive to water contaminants are selected from available stocks and incorporated into a bio-ink formulation with tuned rheological properties (Figure 1a). In the second step, the diatom-laden bio-inks are printed at room temperature into 3D structures using the extrusion bioprinting technique (Figure 1b). This tool allows for the deposition of multiple different inks in a single multimaterial printing approach. Next, the printed structures are incubated into culture media in order to crosslink the hydrogels and, possibly, promote the proliferation of the immobilized diatoms (Figure 1c). Finally, the living sensing device is immersed in a bath of water collected from the source under analysis and the presence of contaminants is assessed (Figure 1d,e). The assessment is based on the extent of proliferation of the diatoms during the incubation period.

In order to explore cells with distinct levels of tolerances toward water contaminants, three diatom species were selected for bioprinting: *Coscinodiscus granii*, *Cyclotella meneghiniana*, and *Fragilaria capucina*. *C. granii* is a marine species with a disc-shaped morphology and large size in the range 40–200 μm (**Figure 2**a).[31] Due to its easy visualization and analysis by op-

tical imaging, we used this species as a model diatom for the bio-ink design and optimization. *F. capucina* (score 3) and *C. meneghiniana* (score 6) were selected because they display very different scores in the water quality assessment scale, allowing us to potentially differentiate the concentration level of contaminants presented in the analyzed water.[32] The scale ranges from one to eight, with the higher values indicating worse water quality (Figure 1e). *F. capucina* are freshwater colonial diatoms that form long ribbons through the attachment of individual cells (Figure 2b),[33,34] whereas *C. meneghiniana* are brackish water species with a cylinder-shaped morphology whose size ranges from 6 to 18 μm (Figure 2c).[35] The selected fresh- and brackish water species are suitable as biological indicators in our platform, since water quality is more commonly investigated in freshwater, such as rivers or ponds.

The bio-ink composition is designed to enable bioprinting of distortion-free structures while also allowing for the proliferation of diatoms entrapped in the hydrogel. To print distortion-free structures, we use cellulose nanocrystals as rheological modifier in combination with sodium alginate for the chemical crosslinking after printing. In the presence of CNCs, the bio-ink is expected to show the shear-thinning behavior, elastic modulus and yield stress required for extrusion bioprinting.[36,37] The crosslinking of the alginate provides stiffness to the hydrogel and prevents its dissolution during incubation of the printed structure during diatom proliferation. Importantly, the biocompatible nature of these bio-ink constituents is essential to ensure cell viability in the printed structures. To promote cell proliferation within the crosslinked hydrogel, a culture medium typically used for diatom growth is utilized as liquid phase of the bio-ink (medium L1).

The rheological behavior of the inks was evaluated to establish the concentration of CNC particles needed to achieve the shear-thinning response, storage modulus and yield stress needed for the extrusion printing process. To this end, we performed oscillatory and steady-shear rheology measurements on cell-free inks prepared with different concentrations of CNC particles and alginate molecules (**Figure 3**a–c). Data obtained from the oscillatory tests indicate that a CNC content of 8 wt% is already sufficient to create a viscoelastic hydrogel with a high storage modulus at rest (G'_0) and a well-defined yield stress (σ_y). Increasing the CNC concentration from 8 to 23 wt% leads to a continuous increase in the storage modulus from 3.9 to 74.6 kPa. This is accompanied by a gradual increase of the yield stress from 97.5 to 269.5 Pa (Figure 3b). Steady-shear measurements reveal the strong shear-thinning responses of inks prepared with CNC concentrations in the range 8–25 wt% (Figure 3c). The shear-thinning behavior of the inks can be described by a power law and is similar to previously reported inks[38] (Figure S1, Supporting Information). In contrast to the effect of CNCs, alginate in the concentration range 0.5–2.0 wt% was found to have no major influence on the rheological properties of the ink (Figure S2, Supporting Information).

Previous research has shown that G'_0 and σ_y values above 10^4 and 100 Pa, respectively, are required to prevent gravity- and capillary-driven distortion of complex-shaped structures printed by extrusion printing.[37,39,40] Because the storage modulus and yield stress obtained with 13 wt% CNC lie close to these values, bio-ink formulations with at least 18 wt% CNC were used to print the diatom-laden living structures. Bioprinting experiments

ADVANCED
SCIENCE NEWS

www.advancedsciencenews.com

NANO · MICRO
small
www.small-journal.com
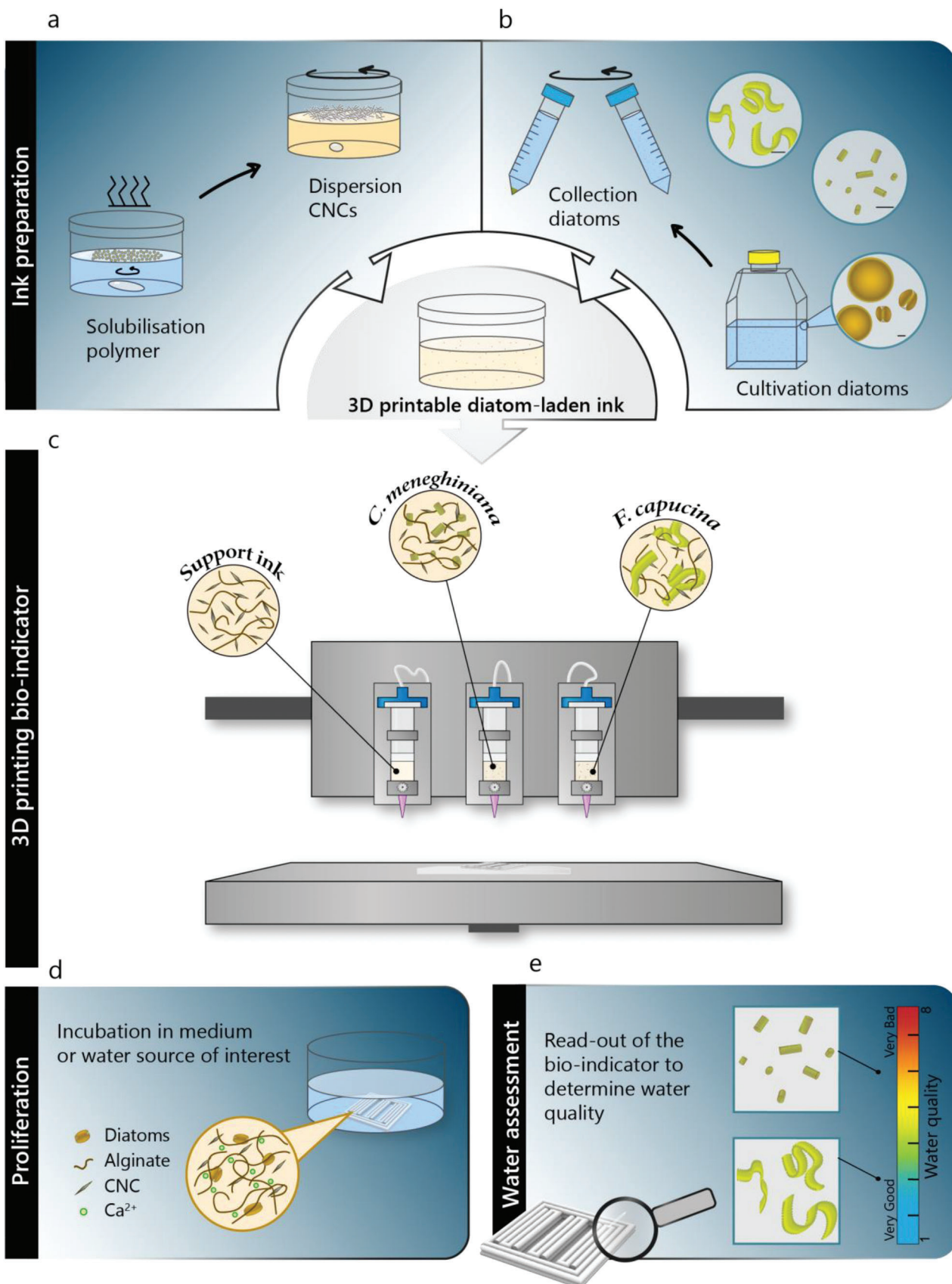
confirmed that structures manufactured from inks with 8 wt% CNC are not stiff enough to impede gravity-induced slumping at the bottom of the print (insets in Figure 3a and Figure S3, Supporting Information). By contrast, formulations with 18 wt% of the rheological additive can be easily printed into high-fidelity, complex-shaped structures (Figure 3d). First qualitative tests with cell-laden bio-ink formulations containing 1.5 wt% alginate show that diatoms remain alive and are able to divide within the printed hydrogels after incubation for 4 days in calcium-containing culture medium (Figure 3d). Based on these results, a bio-ink composition containing 18 wt% CNC and 1.5 wt% sodium alginate was selected as base formulation for diatoms cultured in L1 (enriched seawater) medium (Figure S4, Supporting Information).

The calcium ions provided in the incubation solution allow for the entrapment of diatoms inside the gel via the chemical crosslinking of alginate. The crosslinking effect should be sufficient to minimize diatoms escaping into the incubation medium, while still keeping the gel soft enough to enable cell division and proliferation. To establish the calcium concentration resulting in gels with such intermediate stiffness, we measured the elastic modulus of printed specimens containing different CNC concentrations and crosslinked in aqueous solutions with 10 to 75 mM calcium chloride ($CaCl_2$) (Figure 3e). The experiments reveal that the elastic modulus of the specimens (E) increases markedly upon chemical crosslinking of the alginate molecules when the CNC content is equal or higher than 13 wt%. For a CNC concentration of 13 wt%, the E value increases from 9 to 37 kPa when the $CaCl_2$ concentration is changed from 10 to 75 mM. The effect is amplified in gels containing higher CNC contents. Formulations with 23 wt% CNC, for example, show E values of 25 and 79 kPa for 10 and 75 mM $CaCl_2$, respectively.

For bacterial colonies in previous research, a change in storage modulus of the gels from 20 to 45 kPa was shown to decrease the volume fraction of bacterial colonies by 65 %.[41] To investigate the effect of gel stiffening on the proliferation of diatoms, we measured the growth of *C. granii* in specimens prepared with distinct CNC concentrations after 0, 4, 10, and 21 days of incubation (Figure 3f). Since CNC particles were found to be non-toxic for *C. granii*, the growth of diatoms in specimens containing different nanocellulose contents is expected to be predominantly affected by the elastic modulus of the gel. This is in line with the recent work on bacteria-laden Pluronic-based hydrogels indicating that the average volume fraction and sphericity of bacterial colonies decrease significantly with the increasing elastic modulus of the gel.[41]

While the growth experiments were focused on diatoms entrapped in the hydrogel, it is important to note that cells were also observed to leach into the medium during incubation. This is most likely due to the slight degradation of the hydrogel at the filament edges combined with the expansion of diatom colonies that are located at the boundaries of the hydrogel structure. Diatoms at these locations push the newly formed daughter cells outside of the ink filaments (Figure 3d, Day 4). These free diatoms were noticed to form colonies at a faster pace than inside of all the hydrogel compositions. By exchanging the culture medium every 7 days and washing samples before dissolving and imaging, we ensure that the number of cells counted in our experiment refers only to diatoms that remained entrapped in the hydrogel. This allowed us to capture the effect of the mechanical properties of the hydrogel on diatom growth.

The experimental results show that the presence of CNC particles reduces significantly the growth of diatoms in the hydrogels. An increase in CNC content from 8 to 23 wt% in samples incubated over 21 days leads to a decrease in reached cell density from 22.5×10^3 to 3.8×10^3 cells g^{-1} (Figure 3d). This experimental observation is in agreement with earlier studies on the growth of bacteria or algal cells in gel matrices of distinct stiffnesses.[41–44] The reduced cell proliferation in stiff gels is also observed when the $CaCl_2$ content is increased while keeping the CNC concentration constant (Figure 3g). However, in this case it is not possible to decouple mechanical and chemical effects on diatom proliferation, since $CaCl_2$ concentrations above 50 mM were observed to inhibit diatom growth in toxicity experiments in solution (Figure S5, Supporting Information). In addition to stiffness, the possible limited light penetration and reduced diffusion of nutrients in gels prepared with high CNC concentration might also hinder the proliferation of the immobilized diatoms. Further research is required to quantify the possible contributions of these effects to the limited growth of diatoms in gels with higher CNC contents.

The ability of the diatoms to proliferate also when immobilized in the hydrogels allows us to harness their metabolic activity for water assessment purposes. To illustrate this, we evaluated the growth of two distinct diatom species in the presence of compounds that belong to three typical groups of water contaminants. Sodium chloride (NaCl) was used as an example of salt contamination resulting, among others, from the salt deposited on roads in winter. DCMU (*N*′-(3,4-dichlorophenyl)-*N*,*N*-dimethylurea) and Irgasan (trichloro-2′-hydroxydiphenyl ether) were taken as representatives of herbicides and antimicrobial agents, respectively, two types of compounds often found as contaminants in water. The herbicide prevents the proliferation of algae by blocking the binding site of the protein complex photosystem II, thus inhibiting photosynthesis. The antimicrobial agent kills bacteria and fungi by impeding the action of an enzyme involved in the synthesis of fatty acids in microorganisms. Since the selected diatoms *F. capucina* and *C. meneghiniana* (Figure 2b,c) display different scores in water quality control, we hypothesize that they should also show distinct sensitivities to these herbicide and antimicrobial agents.

To establish the sensitivity of these diatoms to the chosen contaminants, we measured the growth of *F. capucina* and *C. meneghiniana* in aqueous media containing different concentrations

Figure 1. Manufacturing platform for the 3D printing of living diatoms. a) Bio-ink preparation starts through the solubilization of sodium alginate and the dispersion of cellulose nanocrystals (CNC) in L1 (enriched seawater) medium (saline). b) Diatoms are selected and cultivated under specific growth conditions before collection by centrifugation. *Coscinodiscus granii*, *Cyclotella meneghiniana*, and *Fragilaria capucina* are shown as examples of diatom species selected for this study. Scale bars: 20 µm. c) Living bioindicators are 3D printed into customized designs via multi-material extrusion bioprinting of different diatom-laden inks. d) Diatom proliferation occurs through post-printing incubation of the printed objects. e) Water quality assessment proceeds by inspecting the individual responses of the diatom species after incubation in water. The water quality is evaluated based on the known score for the different diatom species.
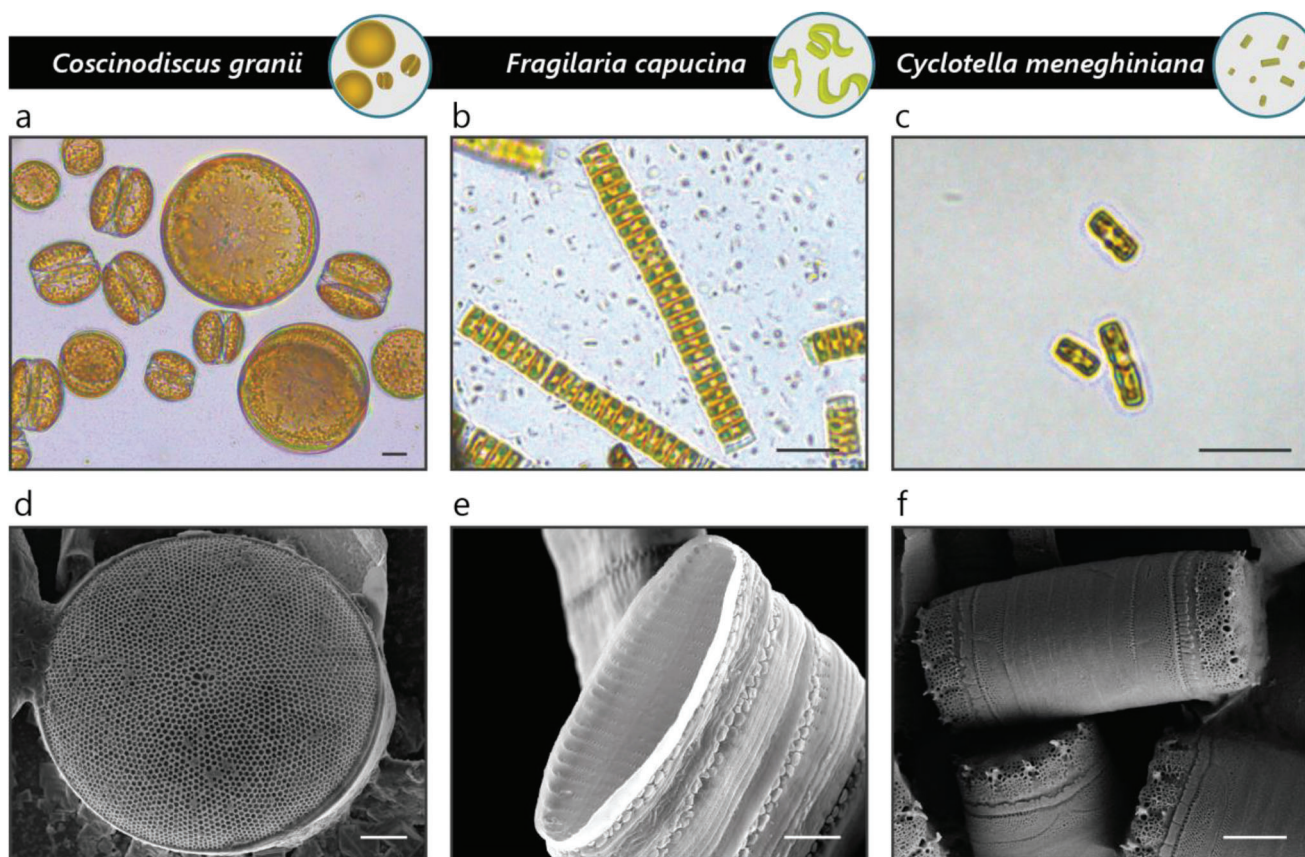
ADVANCED
SCIENCE NEWS
www.advancedsciencenews.com

NANO · MICRO
small
www.small-journal.com

Figure 2. Morphology of selected diatom species. a–c) Optical and d–f) electron microscopy images of a,d) *Coscinodiscus granii*, b,e) *Fragilaria capucina*, and c,f) *Cyclotella meneghiniana*. Scale bars (a–c): 20 µm, d): 10 µm, e,f): 2 µm.

of NaCl, DCMU and Irgasan. First experiments were carried out with free-living suspended diatoms in order to ensure their metabolic activity is not hindered by the entrapment in the hydrogel. Growth was quantified by the autofluorescence of the chlorophyll pigments produced by the diatom for photosynthesis. Samples with varying concentrations of contaminants were cultured in well plates for 14 days before imaging with a fluometric imager (**Figure 4**a). Additionally, fluorescence intensities were regularly measured by a photo-spectrometer (Figure S6, Supporting Information). The concentrations of contaminants were selected to cover the typical range expected in natural aquatic environments.[45–47]

The sensitivity of the diatoms is given by the maximum concentration of salt or contaminant that still allows for the production of chlorophyll, taken here as a measure of the cell's metabolic activity. This is referred to as the maximum acceptable toxicant concentration (MATC). Fluorescence imaging of the liquid cultures quantitatively confirmed the distinct levels of sensitivities of *F. capucina* and *C. meneghiniana* to the selected contaminants. The MATC values obtained from the fluorescence data were defined as the salt and contaminant concentrations required to reduce the fluorescence of the contaminant-free control sample by 50% (Figure 4b).

The results show that the MATC values for NaCl are significantly different for the two diatom species in solution, whereas both microorganisms display comparable sensitivity to the her-

bicide DCMU antimicrobial agent. *C. meneghiniana* can withstand salt concentrations 10^3 times higher than that tolerated by *F. capucina*. The high fluorescence observed for cultures of *C. meneghiniana* with salt concentrations up to 15 g L^{-1} and the dim intensity at low concentrations is consistent with the fact that this species inhabits brackish waters, where the salt content can reach 30 g L^{-1}.[48] By contrast, the fresh-water species *F. capucina* was found to thrive only if the NaCl concentration is kept at 1 g L^{-1} or lower, a condition that is met in this diatom's natural environment. These results meet the expected sensitivities of the organisms and thus validate the protocol used in our experiments. Surprisingly, *C. meneghiniana* tolerates slightly higher dosages of herbicide (DCMU) and even mildly increases its fluorescence when incubated in solutions containing up to 2.33 µg L^{-1} DCMU. This unexpected effect might reflect the blockage of photosystem II inside of the chloroplasts by the herbicide. Such blockage is known to induce stronger fluorescence, which can be used for the detection of herbicides in plants.[49]

Although well-plate experiments with cell suspensions are common practice in biological assays, they do not allow for the portability and convenience of multiplexed sensing devices. In addition to enabling the study of the long-term behavior of gently immobilized microorganisms on a single-cell level, the possibility to print diatom-laden hydrogels into 3D structures opens the opportunity to create upscalable materials for CO$_2$ capture[16] or living indicators for a widespread control of water quality. We
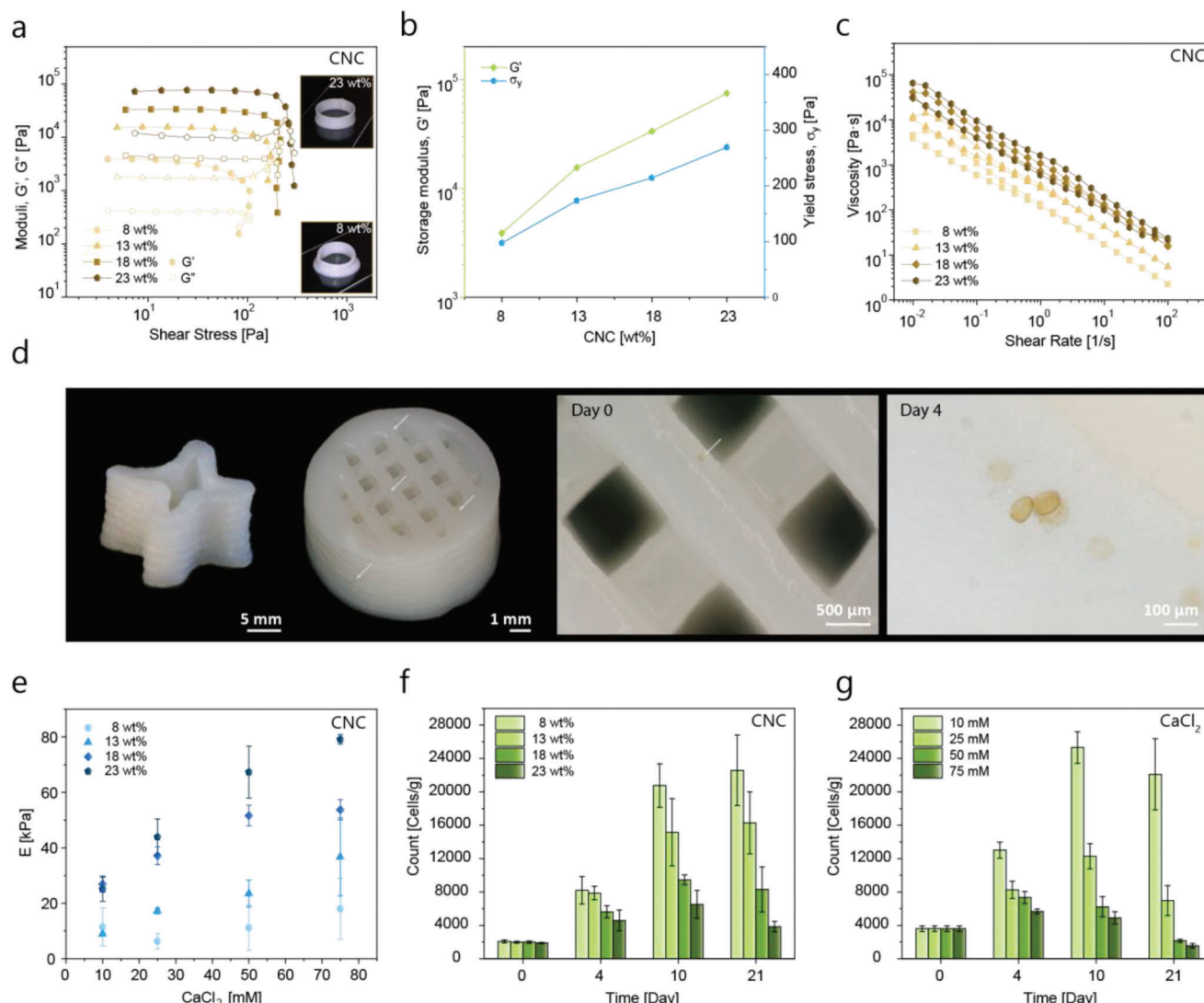
Figure 3. Bio-ink rheology, printability and diatom growth. a) Oscillatory rheological measurements performed at 1 rad s^{-1} for inks containing CNC concentrations between 8 and 23 wt% and fixed sodium alginate content of 1.5 wt%. The data indicate the storage modulus (filled symbols) and loss modulus (open symbols) obtained from amplitude sweeps at a frequency of 1 rad s^{-1}. Hollow cylinders printed from inks prepared with 8 (bottom) and 23 wt% (top) CNC reveal the importance of high CNC concentrations to prevent shape distortion. b) Storage modulus and dynamic yield stress extracted from oscillatory measurements on inks with varying CNC concentrations and constant sodium alginate content of 1.5 wt%. c) Steady-state rheology of inks with distinct CNC concentrations and 1.5 wt% alginate, indicating the strong shear-thinning behavior of all formulations. d) Complex-shaped crosslinked structures printed from diatom-laden inks, highlighting the division of an entrapped *C. granii* diatom after 4 days of incubation in culture medium. White arrows indicate embedded diatoms. e) Effect of the concentration of calcium chloride (CaCl$_2$) in the crosslinking solution on the elastic modulus of cubes printed from inks with different CNC contents. f,g) Evolution of the density of *C. granii* cells inside hydrogel filaments from inks with distinct concentrations of f) CNC particles and g) CaCl$_2$. The growth curves with increasing CNC contents were obtained at constant CaCl$_2$ and alginate concentrations of 10 mM and 1.5 wt%, respectively. For the experimental series with different CaCl$_2$ concentrations, fixed contents of CNC and alginate of 18 and 1.5 wt%, respectively, were used.

explore the potential of the latter by bioprinting hydrogels with more than one diatom species using a multi-material approach. Since *C. meneghiniana* and *F. capucina* display different sensitivities to NaCl, these species can be utilized as independent sensing units in a multiplexed device.

To enable multiple sensing in a single device it is essential to keep the diatoms metabolically active in the hydrogel, while also ensuring physical entrapment to prevent the diffusion and intermixing of the microorganisms. We evaluate whether these conditions can be satisfied in our hydrogels by bioprinting a structure containing both *C. meneghiniana* and *F. capucina* in a specific spatial pattern. The structure was printed using three distinct inks. A cell-free ink with high CNC concentration is used to define the outer contour of the structure. Inks containing either *C. meneghiniana* or *F. capucina* are deposited within this counter to form a simple rectangular pattern.

Optical microscopy of the printed structure reveal that the diatoms do not intermix and remain entrapped within the
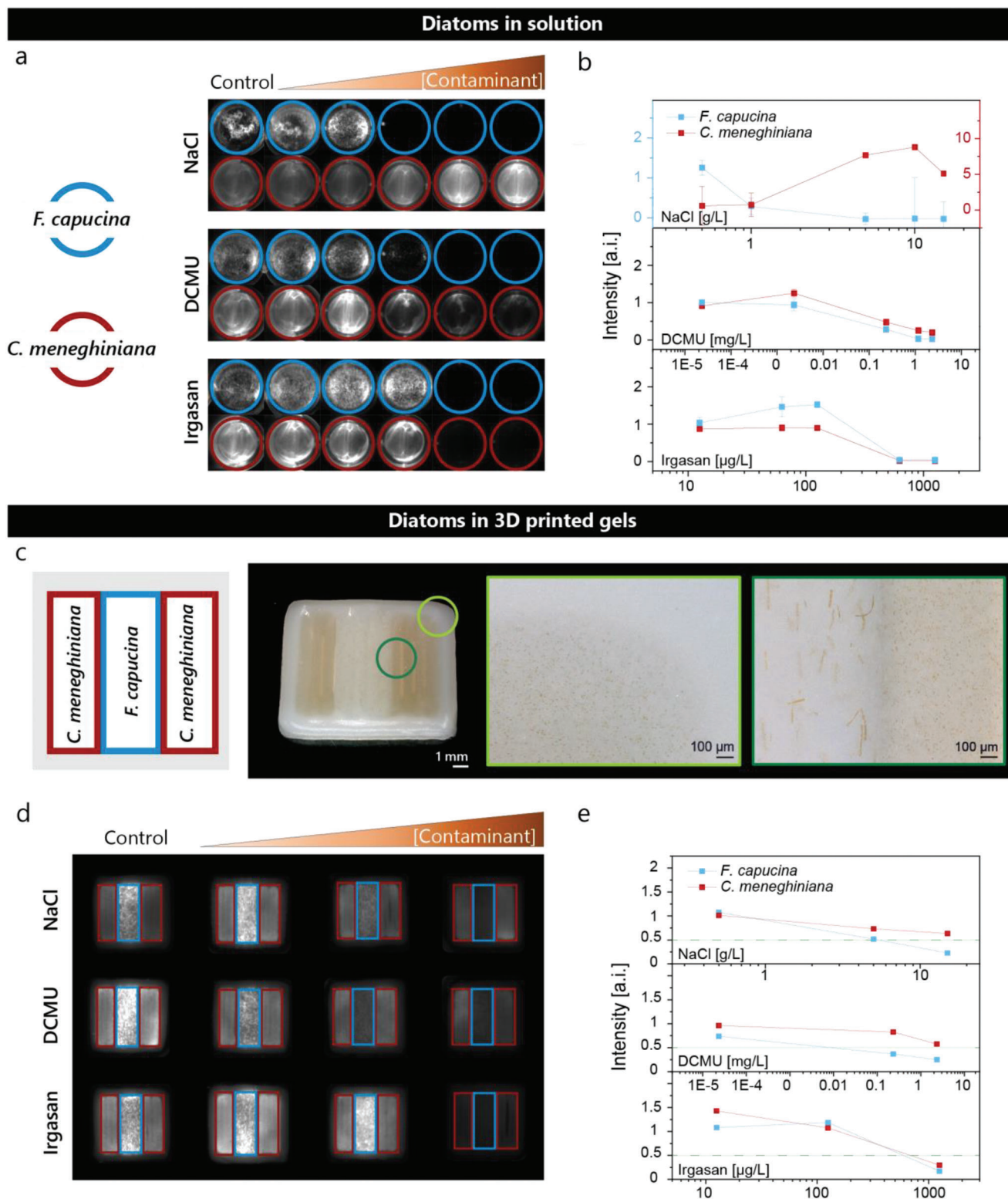
ADVANCED
SCIENCE NEWS
www.advancedsciencenews.com

NANO · MICRO
small
www.small-journal.com

Figure 4. Growth of diatoms in the presence of NaCl or water contaminants. a) Fluorescence images of free *C. meneghiniana* and *F. capucina* grown for 1 week in solutions containing increasing concentrations of NaCl (0.5, 1, 5, 10, 15 g L^{-1}), DCMU (2.33×10^{-5}, 2.33×10^{-3}, 0.233, 1.165, 2.33 mg L^{-1}), and Irgasan (12.5, 62.5, 125, 625, 1250 μg L^{-1}). A control culture without contaminants is shown as a reference. b) Fluorescence intensity obtained from the well-plate experiments, indicating the maximum acceptable toxicant concentrations (MATC) of NaCl, DCMU and Irgasan tolerated by *C. meneghiniana* and *F. capucina* when free in solution. c) Printed hydrogels containing both *F. capucina* and *C. meneghiniana* entrapped in specific locations of the crosslinked gel. In this design, the three regions with entrapped diatoms are surrounded by a stiffer diatom-free ink. The two optical microscopy

rectangular patterns (Figure 4c). To check if they are metabolically active, the printed hydrogels were incubated in media containing different concentrations of salt, herbicide and antimicrobial agents. Fluorescence microscopy of the hydrogels after 14 days of incubation showed that the diatoms display distinct sensitivity profiles compared to that previously observed in the experiments in solution (Figure 4d,e). In our analysis, an intensity value of 50% of that of the control is again considered as the threshold intensity for determining whether the cells are dead or alive, which is taken here as the MATC values (Figure 4d). At the end of the 2 weeks treatment, the intensity variance (standard deviation) between the three identical control samples was 22% and 32% for the compartments with *F. capucina* and *C. meneghiniana*, respectively. Interestingly, *F. capucina* exhibits higher tolerance to salt when immobilized in the gel, which might result from a chemical buffering effect of the gel that reduces the exposure of the diatoms to the salty medium. The immobilization of the diatoms in the gel was also found to hinder the positive effect of NaCl on the growth of *C. meneghiniana*.

In this first proof of concept, the 3D printed bio-indicator allows us to determine whether the diatom species is dead or alive in a yes/no fashion, based on the sensitivity threshold of the chosen species. Hence, three regimes can be distinguished: (yes/yes), meaning that both species are alive and that the concentration is lower than the MATC for both species; (yes/no), when the concentration of contaminant exceeds the MATC of only one species, but is below that of the second species; and (no/no), in which no species survive due to a concentration level above the MATC of both species. Introducing in the tool more species with different sensitivities, such as diatoms and other algae or bacteria, will allow for a more accurate quantification of the presence of contaminants. Overall, our experiments demonstrate that it is possible to effectively immobilize the diatoms in the printed hydrogel without sacrificing their metabolic activity and to assess their differentiated sensitivities to water contaminants.

The differentiated sensitivity of the diatoms to water pollutants was eventually harnessed to print multiplexed living indicators with high surface area and easy visual readout (**Figure 5**). Living indicators with a complex pattern of Gosper curves were first printed using inks containing either *F. capucina* or *C. meneghiniana*. This complex pattern is meant to increase the surface area of the hydrogel and thus facilitate the transport of nutrients and other chemicals to the encapsulated diatoms, thus potentially decreasing the detection time (Figure 5a). To print such a bio-indicator, a cell-free supporting ink with high CNC concentration is first used to generate the contours of the device. The inner space within the contour is then printed with a diatom-laden bio-ink to create the complex pattern.

Fluorescence microscopy images of such devices after 2-week incubation in media with low and high salt concentrations reveal the efficacy of the living material in sensing the presence of NaCl in the water. Hydrogels containing *F. capucina* fluoresce

only at low salt concentrations, whereas structures prepared with *C. meneghiniana* show strong fluorescence independent of the tested amounts of salt in the water (Figure 5b). Here, salt is used to prove the concept. Other chemicals affecting the growth of diatoms with different sensitivities may also be detected using this living material platform.

Next, we combine the two diatom species in a single device to achieve multiplexed sensing (Figure 5c–f). The bio-indicator is fabricated by multi-material bioprinting of two different inks to deposit distinct diatoms in specific regions of the complex pattern. The printing pattern is not limited to the high-surface-area design. Instead, it can benefit from the vast design capabilities of 3D printers, as illustrated here by the alternative diatom-shaped multi-species pattern (Figure 5e,f). Moreover, this alternative design contains the cell-free support ink to define the diatom areas in the device. This lifts the rheological constraints on the diatom-laden inks, simplifying bio-ink design and enabling the deposition of multiple species in the same living bioindicator.

To evaluate the performance of our multiplexed bio-indicator, we used a salt concentration that is tolerated by *C. meneghiniana* but too high to keep *F. capucina* metabolically active. As a result, the region containing *C. meneghiniana* serves as a control, whereas the area loaded with *F. capucina* provides the sensing functionality. When immersed in a solution with reduced salt concentration, both regions of the complex pattern fluoresce, reflecting the metabolic activity of the two diatom types. If the salt concentration is increased beyond the MATC value of *F. capucina*, fluorescence is only observed in regions containing the more salt-tolerant species. Confocal microscopy confirmed the clear difference in sensitivity between the two printed diatom species (Figure S7, Supporting Information). This allows for the assessment of the water salt concentration using a simple classification system (Figure S8a,b, Supporting Information). Notably, the selective proliferation of the diatoms in salty environments is also readily noticed by the naked eye upon visual inspection of the bio-indicator. This easy read-out option should facilitate the widespread use of such a living indicator, since no specialized equipment is necessary for the analysis.

If specialized equipment is available, detection can be achieved in a shorter time range. To demonstrate this, we measured the fluorescence of a multidiatom Gosper bioindicator over time. Experiments in the presence of salt show that the intensity of the compartments with the sensing species (*F. capucina*) decreases to a value below 50% of those in the control medium after 3 days of treatment (Figure 5g,h, Figure S8, Supporting Information). This indicates that it is possible to read out the bioindicator after 3 days, which is in the range of typical liquid toxicity assays.[43–45,50] Furthermore, more specialized tools can also be used for an in-depth study of the microorganism's response at the single-cell level. This enables faster detection in the range of a few hours due to the quick metabolic changes in cells under unfavorable conditions.[51] Further, single-cell studies permit more accurate

---

images show close-up views indicating the clear borders of the different interfaces between diatom-containing and diatom-free regions of the hydrogel. d) Fluorescence images of *C. meneghiniana* and *F. capucina* grown for 2 weeks inside multi-species printed gels exposed to increasing concentrations of NaCl (0.5, 5, 15 g L^{-1}), DCMU (2.33×10^{-5}, 0.233, 2.33 mg L^{-1}) and Irgasan (12.5, 625, 1250 µg L^{-1}). Culture medium without contaminants is shown as a reference (Control). e) Fluorescence intensity obtained from the printed hydrogels, indicating the maximum concentrations of NaCl, DCMU, and Irgasan tolerated by *C. meneghiniana* and *F. capucina* when entrapped in the printed hydrogel (MATC).
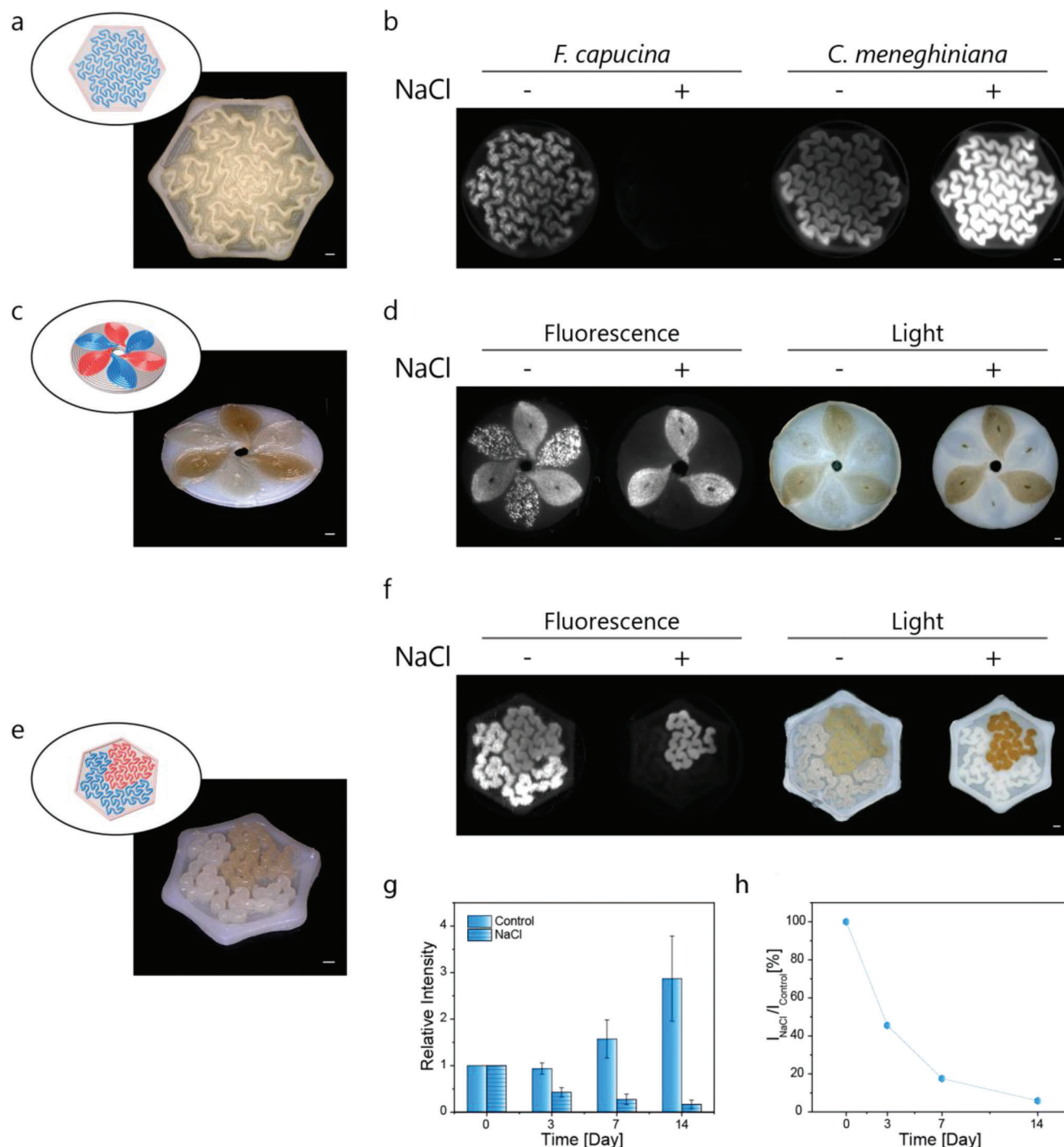
ADVANCED
SCIENCE NEWS
www.advancedsciencenews.com

NANO · MICRO
small
www.small-journal.com

Figure 5. Living bioindicators made by multimaterial bioprinting of diatom-laden hydrogels. a,c,e) Three demonstrators featuring (a) a Gosper curve design using inks containing either *F. capucina* or *C. meneghiniana* diatoms combined with a diatom-free support ink at the edges, (c) a design inspired by a diatom morphology with alternating *F. capucina* or *C. meneghiniana* species, and (e) a multimaterial Gosper design printed with both diatoms. The schematic images in (c) and (e) show the bioindicator design with *F. capucina* in blue and *C. meneghiniana* in red. b,d,f) Light and/or fluorescence microscopy images of the demonstrators after immersion for 14 days in a control Wright Chu (WC)+ medium or in a NaCl-enriched WC+ medium (10 g L^{-1}). Scale bars: 1 mm. g) Evolution of the intensities of the indicator compartments embedding the sensing species *F. capucina* over 14 days after exposure to 10 g L^{-1} NaCl. The graph presents the averaged values of the relative intensities normalized by the gel intensities of the respective gels at day 0 ($n = 5$). The standard deviation of the intensities from all the indicators at day 0 was 33%. h) Ratio between the averaged relative intensities in salt treatment and control condition.

**ADVANCED
SCIENCE NEWS**

www.advancedsciencenews.com

NANO · MICRO

small

www.small-journal.com

detection of cell responses toward varied environmental conditions.

Finally, the broad availability of 3D printers and the biocompatible nature of all bio-ink components facilitates the wide dissemination of the proposed platform. To further develop the bio-indicators, we envision the bioprinting of hydrogels containing a dozen of different diatom species with distinct sensitivities to water contaminants. Such a highly multiplexed device would enable the assessment of water quality using a well-defined index. Similar to the diatom-based Swiss indicator for water quality,[32] the index would be calculated based on the fluorescence of the individual species. This would allow for the assessment of the water quality under the combined effect of multiple contaminants, following a well-established procedure. In contrast to existing diatom-based methodologies, the ease to read out the bio-indicator by non-experts in a quantitative manner similar to a pH strip and the potential to include several species that are relevant for specific environments, makes this a promising, sustainable technology for the development of living sensing devices available for a broad public.

3. Conclusions

Diatom-laden hydrogels can be 3D printed into living bio-indicators for the assessment of waterborne contaminants using a simple visual readout. The hydrogel inks used as feedstock require an optimum concentration of cellulose nanocrystals, sodium alginate and calcium ions in order to achieve the rheological properties needed for extrusion bioprinting while also remaining sufficiently soft and biocompatible to allow for the proliferation of embedded diatoms. Increasing concentrations of cellulose nanocrystals and Ca ions were found to favor bioprinting of distortion-free complex geometries at the cost of a lower growth rate of the diatoms entrapped in the hydrogel. Hydrogels with an optimized formulation enable bioprinting, effective entrapment and differential growth of selected diatoms with distinct sensitivities to water pollutants. Using these optimized inks, we printed portable bio-indicators that can assess the presence of NaCl, herbicide and anti-microbial agent in water by evaluating the number of diatoms proliferated after one to 2 weeks of incubation. Cell proliferation can be quantified from the color and auto-fluorescence of the chlorophyll pigments inside the diatoms by optical microscopy or direct visualization. Our bioprinting platform demonstrates how the metabolic activity of naturally occurring microorganisms can be harnessed to create living functional devices for a societal-relevant application.

4. Experimental Section

Materials: Cellulose nanocrystals (CNC) prepared via sulphuric acid hydrolysis of bleached wood pulp were purchased from CelluForce. Sodium alginate (alginic acid sodium salt, 120–190 g mol^{-1}, 1.56 D-mannuronate : L-guluronate ratio), calcium chloride (CaCl$_2 \geq$ 96%), sodium chloride (NaCl $\geq$ 99.5%), triclosan (Irgasan $\geq$ 97.0%), Dulbecco's phosphate-buffered saline solution (DPBS) and sodium citrate were supplied by Sigma-Aldrich. 3-(3,4-dichlorophenyl)−1,1-dimethylurea (DCMU, 98.0%) was purchased from Tokyo Chemical Industry.

Diatom Cultivation and Collection: A strain of *Coscinodiscus granii* (K-1834) obtained from the Norwegian Culture Collection of Algae (NORCCA,

Norway) was kindly provided by the group of Prof. Eric Dufresne (ETH Zürich, Switzerland). The *C. granii* cells were cultured in L1 medium at 20 °C under 14/10 h light/dark cycles with an irradiance of 100 – 150 µmol photons m^{-2} s^{-1} during the light period. The L1 medium was prepared according to a previously reported protocol.[52] The diatoms were maintained in polystyrene T25 and T75 cell culture flasks closed by filter membrane caps (Techno Plastic Products AG, Switzerland). For experiments, diatoms were collected by centrifuging a certain volume of culture at 1300 RCF for 1 min.

Fragilaria capucina (M2678) and *Cyclotella meneghiniana* (SAG 1020–1) cultures were kindly provided by Marta Reyes (EAWAG Dübendorf, Switzerland). These strains were originally purchased from the Central Collection of Algal Cultures (CCAC, Germany) and from the Department of Experimental Phycology and Culture Collection of Algae (SAG, Germany), respectively. *F. capucina* was cultivated in freshwater WC+ medium,[53] whereas *C. meneghiniana* was kept in 5 g L^{-1} NaCl WC+ medium. Both diatoms species were grown in T25 and T75 flasks and sterilized glass Erlenmeyer flasks at room temperature (23 – 26 °C). Light/dark cycles were imposed during growth by exposing the flasks to normal outside daylight cycles. For cultures with *C. meneghiniana*, flasks were kept shaking at a speed of 140 RPM during growth. *F. capucina* was cultivated in static culture to prevent aggregation. Before collection, the cultures had an optical density at a wavelength of 675 nm (OD$_{675}$) of about 0.06 and 0.04 for *C. meneghiniana* and *F. capucina*, respectively. The cells were collected by overnight sedimentation and/or by centrifuging at speeds over 2000 RCF. For experiments with *C. meneghiniana* in freshwater, the salt medium of the culture was replaced by incubating the cells in pure WC+ medium for several days.

Ink Preparation: The major constituents of the inks were cellulose nanocrystals (CNC) and sodium alginate. To prepare the inks, sodium alginate was first mixed with the appropriate diatom medium at 60 °C for several hours until the sodium alginate was fully dissolved. Next, the CNCs were suspended in the alginate mixture using a planetary mixer (ARE-250, Thinky) at 2000 RPM until a homogeneous dispersion was obtained. A ceramic ball was added to the planetary mixer vessel to improve particle dispersion. Finally, diatoms collected by centrifugation were added to the bio-ink as a suspension (5 wt% of final ink), premixed with a spatula and homogenized by a short planetary mixing step of 30 s to 2 min (2000 RPM) and without the ceramic ball to minimize stresses on the microorganisms.

Ink Rheology: The rheological properties of diatom-free inks were characterized in a stress-controlled rheometer using a 25 mm-sized sand-blasted plate-plate geometry (PP25/S, Anton Paar AG, Switzerland). Storage (G′) and loss (G″) moduli were assessed by applying oscillatory stresses with logarithmically increasing amplitudes at a frequency of 1 rad s^{-1} and at 20 °C. Steady-shear measurements were carried out at the same temperature by applying increasing shear rates from 0.1 to 100 s^{-1} followed by decreasing rates back to 0.1 s^{-1} in order to obtain the flow curves of inks with distinct formulations.

Extrusion Bioprinting and Crosslinking: Inks were 3D printed at room temperature using an extrusion-based desktop printer (3D Discovery, RegenHU Ltd., Switzerland). The 3D designs were created with BioCAD 1.1 (RegenHU Ltd.) and Grasshopper3D (Rhinoceros 3D, v7.0, McNeel Europe). Ready-made inks were loaded into a syringe and centrifuged at 2000 RCF for 1 to 2 min to remove air bubbles. 3D bioprinting was performed using conical polypropylene nozzles with diameters of 0.58 and 0.41 mm. These nozzle diameters are close to the diameter range 0.58–1.6 mm, for which no effect of the nozzle size on cell survival was observed in preliminary experiments. 3D bioprinted structures were immersed in a CaCl$_2$ bath to form a hydrogel via crosslinking of the alginate molecules of the ink. Finally, the diatom-laden hydrogels were incubated in diatom medium or CaCl$_2$-enriched medium under the cultivation conditions described above. The precise crosslinking concentrations and incubation time are provided in the dedicated sections of the respective experiments.

Mechanical Characterisation of Hydrogels: The mechanical properties of the crosslinked hydrogels were tested by compression tests on 3D printed hydrogel cubes of 5 × 5 × 5 mm^3. The three main hydrogel constituents (CNC, alginate and CaCl$_2$) were varied to test their contribution to the mechanical properties. Samples were prepared from inks with

different CNC (8–23 wt%) and alginate (0.5–2 wt%) concentrations, without diatoms. The 3D printed cubes prepared with these inks were crosslinked by immersing the cubes for 4 days in culture medium solutions with a distinct $CaCl_2$ concentration in the range 10–75 mM. This concentration range was chosen to stay below the toxicity threshold (Figure S5c, Supporting Information). The compression tests were performed in a universal mechanical testing machine (Shimadzu AGS-X, Japan) equipped with a 100 N load cell at a displacement rate of 1 mm min^{-1}. Three samples were tested for each experimental condition.

Imaging of Diatoms: Single diatoms and diatoms embedded within the printed filaments were imaged by fluorescence and digital light microscopy (Digital VHX-7000 Keyence microscope, USA). Confocal microscopy (TCS SP8, Leica Microsystems CMS GmbH, Germany) at excitation and emission wavelengths of, respectively, 538 nm and 650–700 nm was also used for diatom visualization, as well as fluorometric imaging (ChemiDoc MP, BioRad Laboratories, Hercules, California) using an excitation wavelength of 650 nm for 0.2 s. The output signal was captured using a light detector after passing the emitted light through a filter cube of 700/50 nm. This visualization technique was additionally employed for automated cell counting of *C. granii* diatoms. The living diatoms were counted by image analysis using an adapted version from the MATLAB trackmen function (MathWorks) written by Maria Kilfoil, which is based on Interactive Data Language code written by John Crocker and David D. Grier.[54] Higher magnification images of the diatoms were obtained by scanning electron microscopy (LEO 1530, Zeiss GmbH, Germany). Before imaging, the diatoms were cleaned with ethanol by applying several centrifugation and resuspension steps. The cleaned diatom frustules were then dried, deposited on carbon tape and coated with a 5–7 nm Pt layer for SEM imaging.

Growth of Immobilized Diatoms: To determine the growth of *C. granii* inside crosslinked hydrogels, the earlier defined inks with varying CNC and sodium alginate contents were mixed with the diatom suspension as described in the ink preparation section. Hand printed filament-shaped samples with a diameter of 0.58 mm were incubated over 21 days in the respective $CaCl_2$ enriched culture medium (10–75 mM). The medium was exchanged weekly to ensure nutrient availability. Cells were counted in samples incubated for 0, 4, 10, and 21 days. The hydrogel filaments were first washed in fresh deionized water and later dissolved in a 0.5 M solution of sodium citrate to enable cell counting. The living cells obtained upon hydrogel dissolution were visualized by fluorometric imaging and counted as described above. Each of the conditions in one experimental series was performed in triplicate, and each experimental series was conducted three times.

Toxicity Assays for Free Diatoms in Liquid Medium: Samples for toxicity assays were prepared by collecting 1-week grown *F. capucina* and *C. meneghiniana* and concentrating the diatoms in water by a factor of 20 before adding 250 µL of the resulting suspension into the 2 mL-volume wells of a 24-well plate (TPP, Switzerland). Solutions of NaCl, DCMU and Irgasan were prepared to evaluate the tolerance of the diatoms toward these chemicals. DCMU and Irgasan solutions were prepared from filtered (0.22 µm) ethanol stock solutions with DCMU and Irgasan concentrations of 20 mM (233 mg L^{-1}) and 100 mg L^{-1}, respectively. 20 µL aliquots of DCMU and 25 µL of Irgasan solutions with concentrations of 10^{-7}, 10^{-5}, 10^{-3}, 5×10^{-3}, and 10^{-2} mM and 1, 5, 10, 50, and 100 mg L^{-1}, respectively, were added to the 2 mL wells containing the diatom suspensions. An autoclaved sterile stock of NaCl-WC was used for the NaCl treatment. The following concentrations of NaCl, DCMU and Irgasan were used in the toxicity assays: 0.5, 1, 5, 10, and 15 g L^{-1} NaCl, 2.33×10^{-5}, 2.33×10^{-3}, 0.233, 1.165, and 2.33 mg L^{-1} DCMU, and 12.5, 62.5, 125, 625, and 1250 µg L^{-1} Irgasan. Diatom growth was quantified by fluorometric imaging, fluorescence emission (435/680 nm excitation/emission) and absorbance (675 nm) in a plate reader (Varioskan Lux, ThermoFisher Scientific, Singapore) over a period of 2 weeks.

Toxicity Assays for Multiple Diatoms Inside Printed Hydrogels: Three different bio-ink formulations were prepared for the 3D bioprinting of the diatom-laden hydrogels. Two of such inks contained 15 wt% CNC, 1.5 wt% alginate and were inoculated either with *C. meneghiniana* or *F. capucina*. The third ink was used for structural support and therefore contained

18 wt% CNC, 1.5 wt% alginate, but no diatoms. A nozzle diameter of 0.58 mm was used for bioprinting rectangular samples of two layers high, including the diatoms at well-defined locations. After printing, the demonstrators were crosslinked for 25 min in a 50 mM $CaCl_2$ solution before washing with phosphate buffer solution (DPBS) and incubation in WC+ medium in static incubation conditions similar as for cultivation. After 3 days of adaptation, the proliferation of *C. meneghiniana* and *F. capucina* entrapped in multi-species hydrogels (Figure 4c–e) was assessed by incubating printed samples in medium with or without contaminant, under static culture conditions in a 12-well plate (TPP, Switzerland) over 2 weeks. The toxicity experiments were performed using the following contaminant concentrations: 0.5, 5, and 15 g L^{-1} NaCl; 2.33×10^{-5}, 0.233, 2.33 mg L^{-1} DCMU; 12.5, 625, and 1250 µg L^{-1} Irgasan; and three control wells containing only WC+ medium. Diatom proliferation was detected by naked eye, optical microscopy using digital and inverted microscopes, as well as fluorometric imaging and confocal microscopy at wavelengths reported above. The intensity of the fluorometric images for each species was extracted with Fiji[55] by measuring the mean intensity of the respective diatom-including gel part divided by the area. Due to the printing design, the area of the *C. meneghiniana* was double the size of that of the *F. capucina*. The average intensity of the identical control samples for each species (n = 3) was used to calculate the relative intensities of the contaminant conditions (n = 1 for each condition).

Multi-Material 3D Bioprinting of Living Bioindicators: Three demonstrator designs were printed with the three inks described above and tested as bioindicators in 10 g L^{-1} NaCl solutions. First, a hexagonal design with an inner pattern based on a Gosper curve was printed with a 0.41 mm sized nozzles. The support ink forms the 2-layer high raft and 5-layer high edges of the printed demonstrator. A continuous print path was used to deposit three layers of the bio-ink containing either *C. meneghiniana* or *F. capucina*. A second demonstrator showed a similar Gosper curve design, but contained both diatoms in a spatially resolved fashion to enable multiplex detection. The third demonstrator was inspired by the frustule pattern of the centric diatom *Actinoptychus senarius*. The frame around the petal-shaped holes of this design was printed with the support CNC-alginate ink (without diatoms) using a 0.41 mm nozzle and subsequently filled by the two diatom-based inks in an alternating manner. The final structure was two layers high. After printing, the demonstrators were treated similar as the gels for the toxicity assays described above. Analysis was performed following a procedure similar to that used for toxicity assays in printed hydrogels with multiple diatoms. The auto-fluorescence of diatom-free gels was used as background signal and subtracted from the measurements with diatom-laden samples. The intensity of the gel compartments was normalized based on their respective intensity at day 0 (n = 5).

Statistical Analysis: Where applicable, tests were executed on three independent samples (n = 3), unless stated differently, and represented as mean ± standard deviation. FIJI and MATLAB were utilized to obtain and analyze the data.

Supporting Information

Supporting Information is available from the Wiley Online Library or from the author.

Acknowledgements

ADVANCED
SCIENCE NEWS

www.advancedsciencenews.com

NANO · MICRO

small

www.small-journal.com

[1] M. Schaffner, P. A. Ruhs, F. Coulter, S. Kilcher, A. R. Studart, *Sci. Adv.* **2017**, *3*, aao6804.

[2] P. Q. Nguyen, N. M. D. Courchesne, A. Duraj-Thatte, P. Praveschotinunt, N. S. Joshi, *Adv. Mater.* **2018**, *30*, 1704847.

[3] J. Caro-Astorga, K. T. Walker, N. Herrera, K.-Y. Lee, T. Ellis, *Nat. Commun.* **2021**, *12*, 5027.

[4] C. Gilbert, T.-C. Tang, W. Ott, B. A. Dorr, W. M. Shaw, G. L. Sun, T. K. Lu, T. Ellis, *Nat. Mater.* **2021**, *20*, 691.

[5] A. M. Duraj-Thatte, N. M. D. Courchesne, P. Praveschotinunt, J. Rutledge, Y. Lee, J. M. Karp, N. S. Joshi, *Adv. Mater.* **2019**, *31*, 1901826.

[6] P. A. Ruhs, K. G. Malollari, M. R. Binelli, R. Crockett, D. W. R. Balkenende, A. R. Studart, P. B. Messersmith, *ACS Nano* **2020**, *14*, 3885.

[7] S. van der Zwaag, N. H. van Dijk, H. M. Jonkers, S. D. Mookhoek, W. G. Sloof, *Philos. Trans. R. Soc. London, Ser. A* **2009**, *367*, 1689.

[8] H. M. Jonkers, E. Schlangen, in *Fracture Mechanics of Concrete and Concrete Structures*, (Eds.: A. Carpinteri, P. G. Gambarova, G. Ferro, G. A. Plizzari), Taylor & Francis Ltd, London **2007**.

[9] S. Sankaran, S. Zhao, C. Muth, J. Paez, A. del Campo, *Advanced Science.* **2018**, *5*, 1800383.

[10] S. Gantenbein, E. Colucci, J. Käch, E. Trachsel, F. B. Coulter, P. A. Rühs, K. Masania, A. R. Studart, *Nat. Mater.* **2022**, *22*, 128.

[11] A. M. Duraj-Thatte, A. Manjula-Basavanna, J. Rutledge, J. Xia, S. Hassan, A. Sourlis, A. G. Rubio, A. Lesha, M. Zenkl, A. Kan, D. A. Weitz, Y. S. Zhang, N. S. Joshi, *Nat. Commun.* **2021**, *12*, 6600.

[12] S. Balasubramanian, K. Yu, A. S. Meyer, E. Karana, M.-E. Aubin-Tam, *Adv. Funct. Mater.* **2021**, *31*, 2170222.

[13] M. R. Binelli, A. Kan, L. E. A. Rozas, G. Pisaturo, N. Prakash, A. R. Studart, *Adv. Mater.* **2022**, *35*, 2207483.

[14] M. R. Binelli, P. A. Rühs, G. Pisaturo, S. Leu, E. Trachsel, A. R. Studart, *Biomater. Adv.* **2022**, *141*, 213095.

[15] A. Lode, F. Krujatz, S. Brüggemeier, M. Quade, K. Schütz, S. Knaack, J. Weber, T. Bley, M. Gelinsky, *Eng. Life Sci.* **2015**, *15*, 177.

[16] S. Malik, J. Hagopian, S. Mohite, C. Lintong, L. Stoffels, S. Giannakopoulos, R. Beckett, C. Leung, J. Ruiz, J. Cruz, B. Parker, *Global Challenges* **2020**, *4*, 1900064.

[17] A. Saha, T. G. Johnston, R. T. Shafranek, C. J. Goodman, J. G. Zalatan, D. W. Storti, M. A. Ganter, A. Nelson, *ACS Appl Mater Interfaces* **2018**, *10*, 13373.

[18] F. Krujatz, S. Dani, J. Windisch, J. Emmermacher, F. Hahn, M. Mosshammer, S. Murthy, J. Steingröwer, T. Walther, M. Kühl, M. Gelinsky, A. Lode, *Biotechnol. Adv.* **2022**, *58*, 107930.

[19] B. A. E. Lehner, D. T. Schmieden, A. S. Meyer, *ACS Synth. Biol.* **2017**, *6*, 1124.

[20] E. A. Guzzi, G. Bovone, M. W. Tibbitt, *Small* **2019**, *15*, 1905421.

[21] Z. Bao, M. R. Weatherspoon, S. Shian, Y. Cai, P. D. Graham, S. M. Allan, G. Ahmad, M. B. Dickerson, B. C. Church, Z. Kang, H. W. Abernathy Iii, C. J. Summers, M. Liu, K. H. Sandhage, *Nature.* **2007**, *446*, 172.

[22] E. V. Armbrust, *Nature* **2009**, *459*, 185.

[23] V. I. Rich, R. M. Maier, in *Environmental Microbiology (Third Edition)*, (Eds.: I. L. Pepper, C. P. Gerba, T. J. Gentry), Academic Press, San Diego **2015**.

[24] J. A. Raven, *Biol. Rev. Camb. Philos. Soc.* **1983**, *58*, 179.

[25] J. Serôdio, J. Lavaud, in *Life Below Water*, (Eds.: W. Leal Filho, A. M. Azul, L. Brandli, A. Lange Salvia, T. Wall), Springer International Publishing, Cham **2020**.

[26] M. G. Kelly, A. Cazaubon, E. Coring, A. Dell'Uomo, L. Ector, B. Goldsmith, H. Guasch, J. Hürlimann, A. Jarlman, B. Kawecka, J. Kwandrans, R. Laugaste, E. A. Lindstrøm, M. Leitao, P. Marvan, J. Padisák, E. Pipp, J. Prygiel, E. Rott, S. Sabater, H. van Dam, J. Vizinet, *J. Appl. Phycol.* **1998**, *10*, 215.

[27] X. Tan, Q. Zhang, M. A. Burford, F. Sheldon, S. E. Bunn, *Front. Microbiol.* **2017**, *8*, 00601.

[28] M. G. Kelly, B. A. Whitton, *J. Appl. Phycol.* **1995**, *7*, 433.

[29] M. Coste, S. Boutry, J. Tison-Rosebery, F. Delmas, *Ecol. Indic.* **2009**, *9*, 621.

[30] J. Richards, J. Tibby, C. Barr, P. Goonan, *Hydrobiologia* **2020**, *847*, 3077.

[31] Coscinodiscus granii, https://www.eoas.ubc.ca/research/phytoplankton/diatoms/centric/coscinodiscus/c_granii.html (accessed: August 2022).

[32] Bundesamt für Umwelt (BAFU), Methoden Zur Untersuchung Und Beurteilung Der Fliessgewässe, https://modul-stufen-konzept.ch/en/diatoms/ (accessed: March 2023).

[33] R. J. Lewis, S. I. Jensen, D. M. DeNicola, V. I. Miller, K. D. Hoagland, S. G. Ernst, *Plant Syst. Evol.* **1997**, *204*, 99.

[34] J. P. Kociolek, S. Blanco, M. Coste, L. Ector, Y. Liu, B. Karthick, M. Kulikovskiy, N. Lundholm, T. Ludwig, M. Potapova, F. Rimet, K. Sabbe, S. Sala, E. Sar, J. Taylor, B. Van de Vijver, C. E. Wetzel, D. M. Williams, A. Witkowski, J. Witkowski, DiatomBase Fragilaria capucina Desmazières, 1830, **2021**, https://www.diatombase.org/aphia.php?p=taxdetails&id=149361, (accessed: August 2022).

[35] S. A. Spaulding, M. G. Potapova, I. W. Bishop, S. S. Lee, T. S. Gasperak, E. Jovanoska, P. C. Furey, M. B. Edlund, *Diatom Res.* **2021**, *36*, 291.

[36] M. K. Hausmann, G. Siqueira, R. Libanori, D. Kokkinis, A. Neels, T. Zimmermann, A. R. Studart, *Adv. Funct. Mater.* **2020**, *30*, 1904127.

[37] G. Siqueira, D. Kokkinis, R. Libanori, M. K. Hausmann, A. S. Gladman, A. Neels, P. Tingaut, T. Zimmermann, J. A. Lewis, A. R. Studart, *Adv. Funct. Mater.* **2017**, *27*, 1604619.

[38] M. K. Hausmann, P. A. Rühs, G. Siqueira, J. Läuger, R. Libanori, T. Zimmermann, A. R. Studart, *ACS Nano* **2018**, *12*, 6926.

[39] D. Kokkinis, M. Schaffner, A. R. Studart, *Nat. Commun.* **2015**, *6*, 8643.

[40] J. E. Smay, J. Cesarano, J. A. Lewis, *Langmuir* **2002**, *18*, 5429.

[41] S. Bhusari, S. Sankaran, A. del Campo, *Adv. Sci.* **2022**, *9*, 2106026.

[42] S. V. Homburg, O. Kruse, A. V. Patel, *J. Biotechnol.* **2019**, *302*, 58.

[43] N. Kandemir, W. Vollmer, N. S. Jakubovics, J. Chen, *Sci. Rep.* **2018**, *8*, 10893.

[44] N. Saha, C. Monge, V. Dulong, C. Picart, K. Glinel, *Biomacromolecules* **2013**, *14*, 520.

[45] T. Ding, K. Lin, L. Bao, M. Yang, J. Li, B. Yang, J. Gan, *Environ. Pollut.* **2018**, *234*, 231.

**ADVANCED
SCIENCE NEWS**

www.advancedsciencenews.com

**NANO · MICRO
small**

www.small-journal.com

[46] B. Chaumet, S. Morin, S. Boutry, N. Mazzella, *Sci. Total Environ.* **2019**, *651*, 1219.

[47] S. M. Ridley, P. Horton, *Z. Naturforsch C Biosci.* **1984**, *39*, 353.

[48] V. Roubeix, C. Lancelot, *Trans. Waters Bull.* **2008**, *2*, 31.

[49] F. E. Dayan, M. L. d. M. Zaccaro, *Pestic. Biochem. Physiol.* **2012**, *102*, 189.

[50] *OECD, Alga, Growth Inhibition Test*, **1984**, p. 14, https://www.oecd.org/chemicalsafety/risk-assessment/1948257.pdf (accessed: March 2023).

[51] C. J. Choi, J. A. Berges, E. B. Young, *Water Res.* **2012**, *46*, 2615.

[52] R. R. L. Guillard, P. E. Hargraves, *Phycologia* **1993**, *32*, 234.

[53] R. R. L. Guillard, C. J. Lorenzen, *J. Phycol.* **1972**, *8*, 10.

[54] J. C. Crocker, D. G. Grier, *J. Colloid Interface Sci.* **1996**, *179*, 298.

[55] J. Schindelin, I. Arganda-Carreras, E. Frise, V. Kaynig, M. Longair, T. Pietzsch, S. Preibisch, C. Rueden, S. Saalfeld, B. Schmid, J.-Y. Tinevez, D. J. White, V. Hartenstein, K. Eliceiri, P. Tomancak, A. Cardona, *Nat. Methods* **2012**, *9*, 676.

2300771 (13 of 13)